Int. J. Heat Mass Transfer. Vol. 31, No. 4, pp. 779–793, 1988
Printed in Great Britain

0017-9310/88 $3.00+0.00
Pergamon Press plc

Combustion and detonation in multi-phase media. Initiation of detonation in dispersed-film systems behind a shock wave

N. N. SMIRNOV
M.V. Lomonosov State University, Department of Mechanics and Mathematics,
119899, Moscow, U.S.S.R.

(*Received* 27 *June* 1986)

Abstract—Consideration is given to the problems of combustion and detonation propagation in heterogeneous media containing an oxidant in the gaseous phase and a fuel in the condensed phase in the form of dispersed particles in the oxidant flow or of a thin film on the channel walls. Detonation in such systems is shown to have a complex unsteady-state structure substantially differing from one-dimensional: the forward detonation front can exhibit mobile discontinuities and can pulsate periodically. A physical model of pulsating and spin detonation in heterogeneous media is developed. A closed system of equations with boundary conditions is composed that makes it possible to mathematically simulate the transition of slow combustion to detonation. The transition process and the detonation determining parameters are calculated numerically. Unsteady-state processes of combustion transition to detonation in dispersed mixtures of air with a hydrocarbon fuel are studied experimentally.

1. INTRODUCTION

HETEROGENEOUS fuel particle-laden gas systems appear in combustion of fuel droplets or of pulverized hydrocarbon fuel in furnace chambers [1] and in pneumatic transport of combustible materials. Gas–film-type heterogeneous systems originate also during the transport of oxidants in pipelines and operation of compressors when various combustible impurities (lubricating oils), occurring in a flow, settle with time on the walls of tubes. Relatively recently, it has become known that combustion of these systems can turn to be unstable [2, 3] and lead to the change-over from the deflagration to the detonation mode. In particular, these processes are responsible for explosions and destruction of equipment in air piston compressors and manifolds [4].

The specifics of dangerously explosive multi-phase systems resides in the fact that in the case of the cross-section mean mass concentration of fuel, being smaller than the lower concentration limit of homogeneous detonation, heterogeneous detonation is possible and it propagates in a stable self-sustaining regime.

The self-sustaining detonation in systems with liquid fuel droplets was studied, e.g. in refs. [3, 5–8]. Detonation in non-mixed two-phase gas–liquid film-type media was first found experimentally in 1952 [9]. Systematic studies were undertaken 10 years later under the guidance of Troshin [4, 10], were continued by Ragland and co-workers [11, 12] and culminated in the creation of the non-one-dimensional unsteady-state model of detonation in non-mixed two-phase systems [13–15] containing secondary shock waves which give rise to periodic pulsations of the leading detonation front.

In 1975 the possibility of spin detonation in non-mixed heterogeneous systems was discovered theoretically in works guided by Zverev [13]. In the same year independent experimental studies under the leadership of Mitrofanov [16] revealed for the first time the existence of spin detonation in heterogeneous air–kerosene systems and allowed the measurement of its main characteristics.

The self-sustaining detonation in heterogeneous systems simultaneously involving droplets and a liquid fuel film on a wall was considered in ref. [17] in which the process of combustion transition into detonation was also investigated.

2. PHYSICAL MODEL OF DETONATION ORIGINATION AND PROPAGATION IN MULTI-PHASE MEDIA

The internal structure of detonation in heterogeneous systems of gaseous oxidant–condensed fuel type differs essentially from the structure of the familiar homogeneous detonation. This difference consists in a much more extended reaction zone sustaining the bow shock wave and in the presence in this zone of strong discontinuities (secondary shock waves) generated by local explosions. This difference in the structure of the detonation zone is explained by the fact that at the initial instant the oxidant and fuel occur in different phases and are non-mixed and therefore not only combustion of the fuel–air mixture takes place behind the bow shock wave, but also the process of mixture formation.

Interphase mass transfer occurs as a result of the thermal and mechanical influence of a gas flow behind

NOMENCLATURE

A	inner cross-sectional area
a	speed of sound
B	parameter of mass transfer
b	exponent in reaction rate law (order of reaction)
C	resistance coefficient
c_p, c_v, c	specific heats
D	mean velocity of detonation wave in heterogeneous systems
d	tube diameter (inner)
d_k	diameter of fuel droplets
e	internal energy of phases
$\mathcal{F}$	zone of possible detonation
F	mean volumetric forces of interphase interaction
f	force of interphase interaction between a single droplet and other phases
g	gravity acceleration
H	specific enthalpy
h_L	specific heat of vapour generation
I	mass inflow into a unit volume by interphase mass transfer
K	kinetic coefficient
k	dimensionless coefficients
$\mathcal{L}\mathcal{L}$	boundary of the zone of possible detonation
$\mathcal{L}_R$	parameter of Reynolds analogy
L	tube length
$\mathcal{M}$	mass of vapours per unit volume
M	Mach number
m	molar mass
$\dot{m}$	rate of mass supply by evaporation and fuel shedding from unit surface area
N	number of components in gaseous phase
Nu	Nusselt number
n	number of particles (droplets) per unit volume
$\dot{n}$	rate of generation of particles per unit surface area
Pr	Prandtl number
p	pressure
Q	mean-volumetric heat removal by interphase interaction
$Q_p(T)$	heat of chemical reaction at pressure p and temperature T
q	heat flux on phase interface
R	universal gas constant
Re	Reynolds number
r	coefficient of temperature recovery
St	Stanton number
T	temperature
t	time
u	gas velocity
W	mass of fuel vapours burning up per unit volume per unit time
We	Weber number
x	coordinate along tube axis
Y	mass concentration of components in gaseous phase
Z	energy release in secondary explosions
z	coordinate along curvilinear axis.

Greek symbols

α	volumetric concentration
β	coefficient of detonation (fuel mass fraction which, together with oxidant, forms a mixture capable of detonating)
γ	specific heat ratio, c_p/c_v
δ	longitudinal size of zone of possible detonation
ε	mean cross-section thickness of fuel film on walls
ζ	smoothing parameter
η	integration variable
κ	coefficient of compressibility
λ	thermal conductivity
μ	dynamic viscosity
ν', ν''	stoichiometric coefficients before and after reaction
ξ	proportionality coefficient
Π	perimeter of inner cross-section of fuel film surface
Π^0	perimeter of tube inner cross-section not wetted with fuel
ρ	density
σ	surface tension coefficient
τ	shear friction induced stress
Φ	zone of detonation products
ϕ_j	stoichiometric relationship determining the mass of the jth component undergoing complete conversion on oxidant unit mass reaction
Ψ	production of particles per unit volume.

Functions

$\delta(t)$	delta function
$\chi(x)$	Heaviside function.

Vectors: $\mathbf{X}$, $\mathbf{A}$, $\mathbf{D}$.

Subscripts

av	Eckert-type average parameters
d	parameters of interphase interaction between dispersed and gaseous phases
f	parameters of interaction between second and third phases (droplets and film)
i	phase number: $i = 1$, gas; $i = 2$, fuel film on tube walls; $i = 3$, fuel droplets in a flow
j	component in gaseous phase: $j = 1$,

	oxidant; $j = N$, fuel; $j = 2,\dots,N-1$, reaction products and inert components
m	effects of added mass
S	parameters of leading wave
T	parameters of interphase interaction between fuel film and tube surface
W	parameters on gas–film interface
μ	viscous effects.

Superscripts

0	parameters on tube surface not wetted with fuel
*	ignition parameters.

a shock wave on the droplets and liquid layer on the inner tube surface. The shedding and atomization of the droplets of fuel, its evaporation and the diffusion of vapours into the oxidant are responsible for the origination of a combustible gas mixture behind the bow wave.

One of the main factors that determine the mode of detonation propagation in two-phase systems is the process of fuel–air mixture formation behind a bow shock wave. This type of detonation is studied with the aid of different models for the mixture formation mechanism. Among these are models of instantaneous shedding, mixing and evaporation of fuel droplets over the entire flow cross-section [18]; the shedding of droplets from the liquid surface due to the formation of surface waves and phase interface instability [19–27]; for relatively thick fuel films at small detonation rates the shedding of droplets is considered to be the main mechanism of mass supply into the boundary layer, while at high (>1000 m s^{-1}) rates an initially combustible mixture is considered to be formed as a result of evaporation and diffusion [24, 25]. The atomization of droplets in shock waves was also identified as the basic governing mechanism in detonation propagation in a gas–droplet medium [3, 7]. In refs. [28–30], the basic mechanism of mixture formation was considered to be evaporation and diffusion of fuel vapours in a boundary layer.

Among theoretical publications that consider detonation in two-phase systems, two groups of works can be distinguished: in one group the authors suggest a purely shedding mechanism of mixture formation [3, 7, 31, 32], in the other a purely diffusion one [33, 40].

In the present author's opinion, both mechanisms of mixture formation should be taken into account. The shedding and atomization of droplets occur some distance down the shock wave and lead to a sharp increase in the interfacial area. At the same time, the formation of the volumes of combustible mixture capable of exploding results from fuel evaporation and mixing of vapours with an oxidant. Also the processes of evaporation and combustion that take place behind the bow shock wave before the origination of perturbations on the surface and start of shedding are essential. It is these processes that determine the fields of temperatures and velocities in gas and liquid against the background of which the perturbations of the surface develop and droplets shed from wave crests.

Thus, on detonation in a heterogeneous medium containing dispersed droplets and a liquid film on the tube walls, phase transitions of various types are possible. First, the fuel can evaporate from the film surface and liquid droplets. Second, there can take place the shedding of fine droplets from the film surface and atomization of large droplets (it is convenient to consider the film and dispersed droplets as different phases). Third, there can take place the deposition of large droplets on the tube surface, film formation and coalescence of small droplets into large ones.

In most cases the ignition of a combustible mixture in a boundary layer takes place at a distance of about 1 cm from the leading wave [41]. Heat liberation during combustion substantially increases the heat flux into the liquid layer and enhances evaporation. In many systems the rate of fuel mass supply into the boundary layer by means of evaporation and shedding of droplets exceeds the rate of combustion, and the fuel accumulates in the boundary layer farther and farther away from the bow shock wave. As a result of this, at a distance of about 10 cm from the bow shock wave, the zone of possible detonation, $\mathscr{F}$, is formed [42, 43] where the conditions develop, as to the concentration limits and critical diameter, which are a prerequisite for detonation propagation in homogeneous media. Thus, inside the structure of heterogeneous detonation, the conditions are created for the propagation of a homogeneous, proper detonation wave. At the edge of the zone of possible detonation, the detonation wave degenerates into a secondary shock wave which overtakes the bow shock wave and serves as the mechanism which transfers energy from the proper detonation wave to the bow wave.

Thus, detonation in a two-phase system is represented by a complex which contains a bow shock wave, an extended zone of reaction with fuel evaporation and combustion, and a proper detonation wave degenerating into a secondary shock wave. The mode of two-phase detonation propagation is determined by the net effect of the flow on the bow shock wave for the period. The flow net effect is determined by the influence of the proper detonation wave (by means of the secondary shock wave and subsequent rarefaction) and also by the influence of weak perturbations, because of the presence of a boundary layer on the tube walls (due to friction, heat fluxes to the walls and fuel layer, evaporation and combustion of fuel) and by the dispersed phase influence (shedding, atomization, acceleration of droplets, warming-up, evaporation and combustion). The self-sustaining mode of detonation propagation in non-mixed systems is determined by the equality of losses and supplies of energy to the bow shock wave for the period, i.e. by the net flow effect being equal to zero.

Depending on the shape of the tube cross-section, different variants are possible for the propagation of the proper detonation wave in non-mixed heterogeneous systems.

In a square duct, when a fuel layer covers one or two opposite walls and, probably, the entire perimeter, the detonation in the zone $\mathscr{F}$ occurs periodically. The subsequent detonation is initiated by secondary shock waves reflected from the opposite tube wall or originating on it [42, 44]. The propagation of heterogeneous detonation is of forced pulsating nature [41].

In a circular duct with a fuel layer covering the entire perimeter, continuous helical propagation of the proper detonation wave is possible in the wall boundary layer (spin detonation in non-mixed systems) [43, 44]. This character of the proper detonation wave propagation (rotation) is explained by the fact that, when propagating in the gas behind the bow shock wave with a supersonic velocity, it should have a subsonic longitudinal velocity component equal to the velocity of the bow shock wave.

Thus, the character of propagation of the proper detonation wave and of the associated secondary shock waves determines two different limiting modes of detonation propagation in non-mixed two-phase systems: pulsating and spin-like. Each of these modes will now be considered in more detail.

In a rectangular duct with one of its walls (lower) covered with a fuel layer the detonation-induced secondary shock wave in the zone $\mathscr{F}$ (Figs. 1(a) and (b)) reaches, while propagating in oxidant, the opposite (upper) wall, reflects from it (Fig. 1(c)) and falls onto the lower wall. For this time the bow shock wave moves a distance δ and the evaporating fuel forms a new zone of possible detonation in the boundary layer on the lower wall $\mathscr{F}$ (Fig. 1(d)) which is located between the bow shock wave and the zone Φ with the detonation products from the previous explosion. Detonation in the newly formed zone $\mathscr{F}$ originates in the case when the intensity of the reflected secondary wave falling onto it is higher than some minimal intensity required for detonation initiation. A new explosion generates a new secondary wave (Fig. 1(e)) which, after being reflected from the upper wall, falls onto the lower wall and initiates explosion in a newly generated zone $\mathscr{F}$. Thus, the process of the formation of secondary waves has a forced periodical character.

With a premixed dispersed phase being present in the flow core, the zone $\mathscr{F}$ can occupy a great portion of the tube section. In this case the flow pattern is close to one-dimensional, secondary waves propagate mainly along the tube axis and the intensity of originating transverse waves is relatively small.

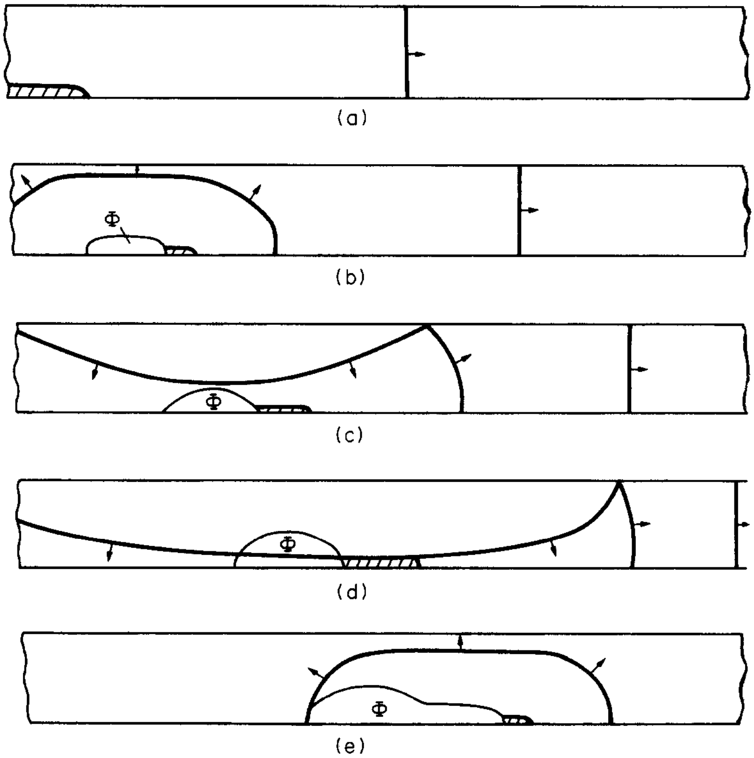

FIG. 1. Scheme of the development of pulsing heterogeneous detonation in gas–fuel film systems.

In circular tubes the entire inner surface of which is covered with a fuel layer, the proper detonation wave moves in a spiral in the zone of possible detonation. In this self-sustaining regime the longitudinal velocity of the proper detonation wave coincides with the bow wave velocity which determines the movement of the possible detonation zone boundary. The velocity of the bow shock wave relative to the gas behind it is subsonic. Since the proper detonation wave propagates with supersonic velocity relative to the gas behind the bow wave and the longitudinal component of its velocity is subsonic, the presence of the transverse velocity component of the proper detonation wave is required for the process to proceed in the steady-state regime.

Outside the zone of possible detonation, a rotating detonation front degenerates into a secondary shock wave which interacts with the bow shock wave on which a discontinuity thus appears which rotates together with the secondary wave.

The pattern of the flow near the tube surface in the system of coordinates $(\tilde{x}, \tilde{z})$ is presented in Fig. 2. The coordinate system is so oriented that the $\tilde{x}$-axis is directed along the tube generatrix, while $\tilde{z}$ is the curvilinear axis of coordinates which is normal to the generatrices and embraces the cylinder around the perimeter. The flow pattern (Fig. 2) is πd-periodical (where d is the diameter of the tube inner cross-section) along the $\tilde{z}$-axis. Here, to the bow shock wave discontinuity there corresponds the branching point C.

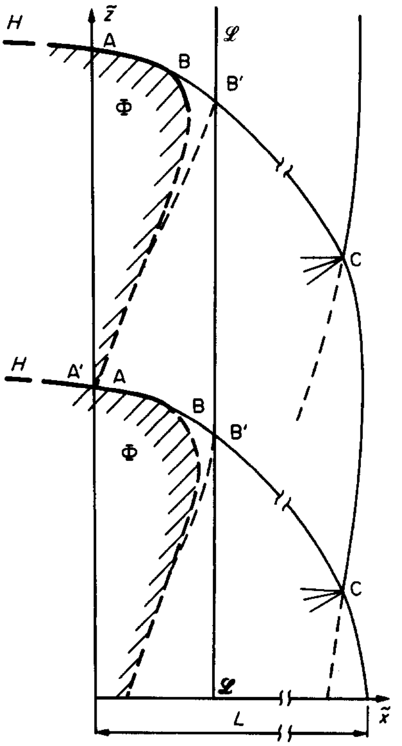

FIG. 2. Flow structure near the tube surface in spin heterogeneous detonation (gaseous oxidant–liquid fuel film).

The system of coordinates $(\tilde{x}, \tilde{z})$ rotates spirally so that the branching point is at rest and gas flows into the system of waves formed at some angle with the $\tilde{x}$-axis. The leading edge of the zone of possible detonation is conventionally shown by the straight line $\mathscr{L}\mathscr{L}$. The front of the proper detonation wave AB passes into the secondary shock wave BC. Over the stretch BB′ the zone of chemical reaction BA′ lags behind the shock front [42–44]. The trajectory of particles intersecting the transverse wave AC at point B′ is conventionally shown by the dashed line B′A′. It is the demarcation between the combustible mixture, which will fully react by the time the proper detonation wave completes its one revolution and the mixture which will start to react during the consequent revolution of the proper detonation wave AB (wave A′B′ in Fig. 2).

3. MATHEMATICAL MODEL OF THE PROCESS

Consider the process of combustion and detonation propagation in a long tube ($L \gg d$) filled with a gaseous oxidant with suspended fuel droplets and having a thin fuel layer on the inner surface. The problem will be solved within the framework of the unsteady-state one-dimensional model. Such a model does not take into account non-one-dimensional effects of the flow structure in the reaction zone, but makes it possible to determine flow integral characteristics with a sufficient degree of accuracy.

Consider a heterogeneous system incorporating three phases: $i = 1$, gas phase; $i = 2$, fuel film on the inner tube surface; $i = 3$, condensed fuel dispersed in a flow. In the case of a large scatter in the size of droplets, the introduction of fine-dispersed (fog) and large-dispersed condensed phases ($i = 3,\dot{3}$) is possible. The condensed phase is considered to be incompressible ($\rho_2 = \rho_3 = \rho = \text{const.}$).

The law of mass flow variation for each phase is formulated as

$$\frac{\partial \rho_1 \alpha_1}{\partial t} + \frac{\partial \rho_1 \alpha_1 u_1}{\partial x} = I_W + I_d \tag{1}$$

$$\frac{\partial \rho \alpha_2}{\partial t} + \frac{\partial \rho \alpha_2 u_2}{\partial x} = -I_W - I_f \tag{2}$$

$$\frac{\partial \rho \alpha_3}{\partial t} + \frac{\partial \rho \alpha_3 u_3}{\partial x} = I_f - I_d \tag{3}$$

where ρ, u, α are the density, velocity and volumetric concentration of phases; I_W, I_d, I_f are the mass inflow per volume unit due to evaporation from the film surface, evaporation of droplets and shedding of particles from the walls, respectively. Atomization, agglomeration and settling of particles are not incorporated in this formulation. Assuming the mean volumetric concentration of the dispersed phase to be small ($\alpha_3 \ll 1$; $\alpha_1 \approx 1-\alpha_2$), determine the mass inflow

$$I_W = \frac{\dot{m}_W \Pi}{A_0}; \quad I_d = \dot{m}_d \frac{6\alpha_3}{d_k}; \quad I_f = \frac{\dot{m}_f \Pi}{A_0};$$

$$\frac{\Pi}{A_0} = \frac{\Pi}{A}\frac{A}{A_0} = \frac{4\alpha_1}{d-2\varepsilon} \quad (4)$$

where A_0, d are the area and diameter of the tube inner cross-section; Π the inner perimeter of the fuel film surface cross-section; d_k the mean diameter of droplets; $\dot{m}$ the rate of mass supply as a result of evaporation or shedding from the unit surface area; ε the average cross-section thickness of the film on the walls.

The law of momentum flux variation is written as

$$\frac{\partial \rho_1 \alpha_1 u_1}{\partial t} + \frac{\partial \rho_1 \alpha_1 u_1^2}{\partial x} = -\alpha_1 \frac{\partial p_1}{\partial x} - F_W - F_0 - F_d - F_f + I_W u_W + I_d u_3 \quad (5)$$

$$\frac{\partial \rho \alpha_2 u_2}{\partial t} + \frac{\partial \rho \alpha_2 u_2^2}{\partial x} = -\alpha_2 \frac{\partial p_1}{\partial x} + F_W + F_f - F_T - I_W u_W - I_f u_W \quad (6)$$

$$\frac{\partial \rho \alpha_3 u_3}{\partial t} + \frac{\partial \rho \alpha_3 u_3^2}{\partial x} = -\alpha_3 \frac{\partial p_1}{\partial x} + F_d - I_d u_3 + I_f u_W. \quad (7)$$

When deriving equations (5)–(7), the change in pressure on the phase interface was neglected ($p_1 = p_2 = p_3 = p$), collisions and agglomeration of particles were not considered. The mean volumetric forces of interphase interaction are determined by the relations

$$F_W = \frac{\tau_W \Pi}{A_0}, \quad F_0 = \frac{\tau_W^0 \Pi^0}{A_0}, \quad F_d = f_d \cdot n = \frac{6\alpha_3 f_d}{\pi d_k^3},$$

$$F_f = f_k \frac{6\dot{m}_f}{\pi d_f^3 \rho}, \quad F_T = \frac{\tau_T \Pi_T}{A_0}$$

where τ_T, τ_W^0, τ_W are the friction-induced stress on the tube surface wetted with fuel, on a dry surface and on the gas–film interface, respectively; Π^0, Π_T the perimeter of the tube inner cross-section not wetted and wetted with fuel; f_d the interphase force acting on a single spherical particle in the gas flow; n the number of particles per unit volume; f_k the pulse of the force of interaction between the film and a droplet during flow separation; u_W the fluid velocity on the gas–film interface.

Note that with no liquid flow in the film, i.e. the velocity $u_W = \text{const.}$ being different from zero only in a mobile coordinate system, equation (6) is greatly simplified. Multiplication of equation (2) by u_W and subtraction from equation (6) yields the statics equation

$$\alpha_2 \frac{\partial p}{\partial x} = F_W + F_f - F_T \quad (8)$$

which can be eliminated from the system since it determines the unknown reaction F_T.

The law of the variation in the number of particles n will be written in the form

$$\frac{\partial n}{\partial t} + \frac{\partial u_3 n}{\partial x} = \Psi.$$

Neglecting the agglomeration and atomization of particles, determine the birth of particles as a result of film destruction Ψ (Weber numbers for particles are 10^3 smaller than for a film): $\Psi = \dot{n}\Pi/A_0$, $\dot{n} = 6m_f/(\pi d_f^3 \rho)$, d_f is the diameter of shedded particles which is assumed to be constant.

The energy equations for each phase have the form

$$\frac{\partial \rho_1 \alpha_1 (e_1 + u_1^2/2)}{\partial t} + \frac{\partial}{\partial x}\rho_1 \alpha_1 u_1 \left(e_1 + \frac{u_1^2}{2} + \frac{p_1}{\rho_1}\right) = -Q_W - Q_d - Q_0 + W\Delta H - F_W u_W - F_0 u_0 - F_d u_3 - F_f u_W + I_W \left(e_W + \frac{p_1}{\rho} + \frac{u_W^2}{2}\right) + I_d \left(e_W + \frac{p_1}{\rho} + \frac{u_3^2}{2}\right) + Z \quad (9)$$

$$\frac{\partial \rho \alpha_2 (e_2 + u_2^2/2)}{\partial t} + \frac{\partial}{\partial x}\rho \alpha_2 u_2 \left(e_2 + \frac{u_2^2}{2} + \frac{p_1}{\rho}\right) = Q_W - Q_T + F_W u_W + F_f u_W - F_T u_0 - I_W \left(e_W + \frac{p_1}{\rho} + \frac{u_W^2}{2}\right) - I_f \left(e_W + \frac{p_1}{\rho} + \frac{u_W^2}{2}\right) \quad (10)$$

$$\frac{\partial \rho \alpha_3 (e_3 + u_3^2/2)}{\partial t} + \frac{\partial}{\partial x}\rho \alpha_3 u_3 \left(e_3 + \frac{u_3^2}{2} + \frac{p_1}{\rho}\right) = Q_d + F_d u_3 - I_d \left(e_W + \frac{p_1}{\rho} + \frac{u_3^2}{2}\right) \quad (11)$$

where u_0 is the velocity of the tube walls different from zero only in a mobile coordinate system; in the majority of problems $u_0 = u_W = u_2 = 0$ in a laboratory system; e_i the internal energy of the ith phase (without allowance for the chemical energy): $e_1 = \hat{c}_v T_1$, $e_2 = cT_2$, $e_3 = cT_3$, $e_W = c_{vW} T_W$; T_W the phase interface temperature; ΔH the specific heat of fuel combustion; W the mass of fuel vapours burnt per unit volume per unit time. The interphase heat transfer is accounted for by the formulae

$$Q_W = \frac{q_W \Pi}{A_0}; \quad Q_0 = \frac{q_W^0 \Pi^0}{A_0}; \quad Q_T = \frac{q_T \Pi_T}{A_0};$$

$$Q_d = \pi d_k^2 n q_d = \frac{6\alpha_3 q_d}{d_k} \quad (12)$$

where q_W^0, q_W, q_d, q_T are the heat fluxes from gas into the wall, fuel layer and into the droplets and from the fuel layer into the wall, respectively.

The function $Z(x, t)$ in equation (9) determines energy liberation on secondary explosions

$$Z = \beta \mathcal{M}_N \Delta H \delta(t - k t_D) \chi(x - x_k) \chi(x_k + \delta - x)/\delta \quad (13a)$$

where $\delta(t)$ is the delta function; $\chi(x)$ the Heaviside function

$$\int_t^{t+\Delta t} Z\,\mathrm{d}t = \begin{cases} \beta \mathscr{M}_N \Delta H/\delta : kt_\mathrm{D} \in [t, t+\Delta t]; \\ \quad x \in [x_k, x_k+\delta], k = 1,2,3,\ldots \\ 0 : kt_\mathrm{D} \notin [t, t+\Delta t], \\ \quad k = 1,2,3,\ldots \\ 0 : \forall x \notin [x_k, x_k+\delta]; kt_\mathrm{D} \in [t, t+\Delta t], \\ \quad k = 1,2,3,\ldots \end{cases} \tag{13b}$$

where t_D is the detonation period, δ the linear dimension of the zone of possible detonation; $\mathscr{M}_N$ the mass of fuel vapours per unit volume at $t = kt_\mathrm{D}$ which are capable of reacting with an oxidant; β the detonation coefficient (fuel mass fraction composing, with an oxidant, a mixture capable of detonating); $x_k = x_k(t)$ the given function which depends on the propagation of the bow shock wave and on the formation of zones of possible detonation.

The system of equations (9)–(11) can be greatly simplified assuming, for example, $u_0 = u_2 = u_W = 0$ (the wall is at rest) and $u_3 = u_1$. Note that equations (10) and (11) serve only for determining the unknown temperature of the condensed phase. In many problems this temperature can be found from additional considerations and there is no need in their solution. For example, when considering rapidly progressing processes, the heat fluxes from the gas into the droplets, fuel film and tube walls can be determined on the assumption that the temperature inside the droplets and the film remain invariable. Then equation (9) can be solved independently.

The gas phase ($i = 1$) is a mixture of chemically reacting gases (components). Each component in the gas phase has the concentration Y_j ($j = 1, \ldots, N$), where the subscript $j = 1$ corresponds to an oxidant, $j = N$ to a fuel, $j = 2, \ldots, N-1$ to reaction products and inert components. To close the system of equations, it is necessary, along with the continuity equation (1) for the entire mixture, to write the equations of mass change for the components:

$$\frac{\partial \rho_1 \alpha_1 Y_j}{\partial t} + \frac{\partial \rho_1 \alpha_1 Y_j u_1}{\partial x} = \begin{cases} W_j + Z_j/\Delta H; j = 1, \ldots, N-1 \\ -W + I_W + I_d - Z/\Delta H; j = N. \end{cases} \tag{14}$$

When deriving equation (14), the one-component nature of the condensed phase was taken into account. The determination of the mass rate of fuel combustion depends on the properties of a heterogeneous system. At relatively small rates of chemical reactions and high rates of fuel evaporation and mixing with an oxidant (high rate of diffusion) a combustible mixture is formed in a gas phase, and the kinetics of chemical reactions turns to be the limiting factor. The reaction rate W is determined by the relation

$$W = \rho_1 \alpha_1 Y_N^b Y_1^{b_1} K(p_1, T_1)\,\mathrm{e}^{-(E/RT_1)}. \tag{15}$$

To this case there corresponds combustion of fine micrometre particles when diffusional gradients are so great that the rates of diffusional and kinetic processes become commensurable.

At high reaction rates, slow evaporation and mixing of fuel with an oxidant and sufficient space between particles, each particle burns with its own microflame and the rate of the combustion process is limited by diffusion. In this case the rate of diffusional combustion W is proportional to the evaporation rate of particles, and in the steady-state regime these rates are equal

$$W = W_1 + W_2$$

$$= \begin{cases} \xi_1 I_W + \xi_2 I_d & \text{when} \quad Y_1 \geqslant Y_* \bigcap T_1 \geqslant T_* \\ 0 + 0 & \text{when} \quad Y_1 < Y_* \bigcup T_1 < T_*. \end{cases} \tag{16}$$

The combustion rates for the rest components W_j, just as the rates of their explosive formation Z_j in equation (14), are determined from equations (13), (15) and (16) by multiplying the values W and Z by the corresponding stoichiometric ratios $(-\phi_j/\phi_N)$.

The mass of fuel vapours per unit volume $\mathscr{M}_N$ in equation (13) is determined from the formula

$$\mathscr{M}_N = \begin{cases} \rho_1 \alpha_1 Y_N & \text{when} \quad Y_N \leqslant \phi_N Y_1 \\ \rho_1 \alpha_1 Y_1 \phi_N & \text{when} \quad Y_N > \phi_N Y_1 \end{cases} \tag{17}$$

where the upper line corresponds to the excess of an oxidant and the lower to the fuel excess.

Thus, a closed system of equations has been obtained which makes it possible to find the solution of the non-stationary problem of combustion and detonation propagation in heterogeneous systems on the assignment of the corresponding parameters of the interphase interaction, detonation period and size of the secondary explosion zone.

4. DETERMINATION OF THE PARAMETERS OF INTERPHASE INTERACTION

The parameters of friction, equation (8), and of the interphase heat and mass transfer, equations (12) and (4), are determining for combustion and detonation propagation in heterogeneous systems. Their values depend, in particular, on the intensity of phase transition and on the presence of chemical reactions near the phase interface in the case of heterogeneous and diffusional combustion and can be determined by solving two-dimensional stationary [45] or one-dimensional non-stationary [46] problems of interphase heat and mass transfer.

The friction force τ_W^0 acting on the inner surface of a cylindrical channel is determined by the relation

$$\tau_W^0 = C_\mathrm{f} \frac{\rho_1 (u_1 - u_W)^2}{2} \tag{18}$$

where u_W is the velocity of the lateral phase interface. The friction coefficient C_f is determined depending on the flow mode

$$C_f = \begin{cases} \dfrac{16}{Re}; \; Re < 1200 \\ \dfrac{0.079}{Re^{1/4}}\kappa^{1/2}; \; 1200 < Re < 10^5 \\ \dfrac{0.074}{Re^{1/5}}\kappa^{3/5}; \; 10^5 < Re < 5\times 10^6 \\ \dfrac{0.033}{Re^{1/7}}\kappa^{5/7}; \; Re > 5\times 10^6 \end{cases} \tag{19}$$

where $Re_W = \rho_1|u_1 - u_W|d/\mu_1$ is the Reynolds number, d the inner diameter of the channel, κ the coefficient accounting for the gas compressibility. Assuming the dynamic viscosity coefficient μ to be directly proportional to the temperature, the following approximate formula is obtained for determining κ:

$$\kappa = \begin{cases} 1, & M_{12} = \dfrac{|u_1 - u_2|}{a_1} \lesssim 1 \\ \dfrac{T_1}{T_{av}}, & M_{12} = \dfrac{|u_1 - u_2|}{a_1} > 1 \end{cases} \tag{20}$$

where T_{av} is the average temperature according to Eckert. Assuming $T_{av} = (T_1 + T_W)/2$, obtain

$$\kappa = \frac{2}{2 + r_B \dfrac{\gamma - 1}{2} M_{12}^2} \tag{21}$$

where r_B is the coefficient of temperature recovery on the channel inner surface, γ the specific heat ratio.

The force f_d acting on a single particle of the dispersed phase in its non-stationary motion is in the general case the sum of the quasi-stationary force of viscous friction f_μ, added mass force f_m and of the 'hereditary' (due to the non-stationary state of the viscous boundary layer around particles) Bassé force f_B [47]

$$f_d = f_\mu + f_m + f_B$$

$$f_\mu^0 = C_\mu^0 \tfrac{1}{2}\rho_1 (u_1 - u_3)^2 \pi d_k^2 \tag{22}$$

where d_k is the particle diameter, C_μ the resistance coefficient

$$C_\mu^0 = \begin{cases} \dfrac{24}{Re_d}\left(1 + \dfrac{3}{16}Re_d - \dfrac{19}{1280}Re_d^2\right); \; Re \lesssim 1.5 \\ \left(\dfrac{24}{Re_d} + \dfrac{4.4}{\sqrt{Re_d}} + 0.42\right)\kappa_1; \; 1.5 < Re < 10^5 \\ 0.21\left(\dfrac{\beta_s d_k}{|u_1 - u_3|}\right)^{4/5} Re_d^{-1/5}\kappa_1; \; Re > 10^5 \end{cases} \tag{23}$$

where

$$\kappa_1 = \left(\frac{\rho_W}{\rho_1}\right)^{4/5}\left(\frac{\mu_W}{\mu_1}\right)^{1/5};$$

$$\beta_s = \frac{|u_1 - u_3|}{d_k} 2\sqrt{\left[\frac{\rho_1}{\rho_s}\left(2 - \frac{\rho_1}{\rho_s}\right)\right]};$$

$$Re_d = \frac{\rho_1 |u_1 - u_3| d_k}{\mu_1};$$

$$\rho_W = \rho_1(T_W, p_1); \quad \mu_W = \mu_1(T_W);$$

$$\frac{\rho_s}{\rho_1} = \begin{cases} \left(1 + \dfrac{\gamma - 1}{2}M_{13}^2\right)^{1/(\gamma - 1)}; \\ \quad M_{13} = \dfrac{|u_1 - u_3|}{a_1} < 1 \\ \dfrac{(\gamma + 1)M_{13}^2}{(\gamma - 1)M_{13}^2 + 2}\left[1 + \dfrac{\gamma - 1}{2} \right. \\ \quad \left. \times \dfrac{(\gamma - 1)M_{13}^2 + 2}{2\gamma M_{13}^2 - (\gamma - 1)}\right]^{1/(\gamma - 1)}; \; M_{13} > 1. \end{cases} \tag{24}$$

Equations (23) can be used to determine the friction force in a dispersed mixture with a relatively small volumetric content of the dispersed phase $\alpha_3/(\alpha_1 + \alpha_3) \leqslant 0.08$. At higher values of α_3 the friction coefficient can be determined from the formula

$$C_\mu = \begin{cases} C_1 = \left(\dfrac{24}{Re_d} + \dfrac{4.4}{Re_d^{0.5}} + 0.42\right)\kappa_1, \\ \dfrac{\alpha_3}{\alpha_1 + \alpha_3} \leqslant 0.08, \\ C_2 = \dfrac{4(\alpha_1 + \alpha_3)}{3\alpha_1}\left(1.75 + \dfrac{150\alpha_3}{\alpha_1 Re_d}\right)\kappa_1; \\ \dfrac{\alpha_3}{\alpha_1 + \alpha_3} \geqslant 0.45 \\ \dfrac{(0.92\alpha_3 - 0.08\alpha_1)C_2 + (0.45\alpha_1 - 0.55\alpha_3)C_1}{0.37(\alpha_1 + \alpha_3)} \\ \quad 0.08 < \dfrac{\alpha_3}{\alpha_1 + \alpha_3} < 0.45. \end{cases} \tag{25}$$

The rest forces involved in equations (25) are determined by the relations [47, 48]

$$f_m = \tfrac{2}{3}\pi d_k^3 \rho_1 \left[\frac{\partial(u_1 - u_3)}{\partial t} + u_1 \frac{\partial u_1}{\partial x} - u_3 \frac{\partial u_3}{\partial x}\right] \tag{26}$$

$$f_B = 6d_k\sqrt{(\pi\rho_1 u_1)} \int_{-\infty}^{t} \frac{\mathrm{d}}{\mathrm{d}t}(u_1 - u_3)\frac{\mathrm{d}z}{\sqrt{(t - z)}}. \tag{27}$$

The heat flux from the gas to the cylindrical channel surface is determined from the relation

$$q_W = \begin{cases} \dfrac{2\lambda_1}{d}(T_1 - T_W) + \dfrac{\mu_1(u_1 - u_W)^2}{d}; & (28) \\ \quad Re \leqslant 1200 \\ \rho_1 u_1 \, St(H_{1r} - H_W + W_1 \Delta H); & (29) \\ \quad Re > 1200 \end{cases}$$

where

$$H_{1r} = c_{p1}T_1 + r\frac{(u_1-u_W)^2}{2};$$

$H_W = c_{pW}T_W$; $W_1\Delta H$ is the chemical energy released during combustion in the wall boundary layer. The Stanton number in equation (28) is determined from the Reynolds analogy

$$St = \tfrac{1}{2}C_f\mathscr{L}_R \tag{30}$$

where C_f is prescribed by equations (19); the recovery coefficient r and the parameter of the Reynolds analogy $\mathscr{L}_R$ are found from

$r \approx Pr^{1/3}$; $\mathscr{L}_R \approx Pr^{-2/3}$ or

$$\mathscr{L}_R = \left[1+11.6(Pr-1)\sqrt{\left(\frac{C_f}{2}\right)}\right]^{-1}$$

where $Pr = \mu_1 c_{p1}/\lambda_1$ is the Prandtl number. Heat exchange between the gas and the dispersed particles is assigned by the relations

$$q = \pi d_k\lambda_1 Nu_d(T_1-T_3) \tag{31}$$

$$Nu_d = \begin{cases} 2+0.106Re_d\,Pr^{1/3};\ Re < 100 \\ 2+0.16Re_d^{2/3}\,Pr^{1/3};\ 100 < Re < 1000 \\ 2+0.03Re_d^{0.54}\,Pr^{0.33}+0.35Re_d^{0.8}\,Pr^{0.36}; \\ \quad Re > 10^3. \end{cases}$$

Equations (19), (23), and (25) describe the interphase friction in the absence of mass transfer well. The presence of substance injection from the phase interface appreciably changes the friction and heat transfer parameters. The influence of injection on the friction on a flat plate τ_W is given by

$$\frac{\tau_W}{\tau_W^0} = \frac{\ln(1+B)}{B};\quad B = \frac{\dot m_W|u_1-u_W|}{|\tau_W|}. \tag{32}$$

Superscript '0' corresponds to the values of parameters in the absence of injection. Equation (32) is derived assuming the flow mode in the wall region similar to the Couette flow $|\partial/\partial x| \ll |\partial/\partial y|$. Numerical calculations [49] showed that equation (32) is a good approximation of the function $\tau_W(B)$ for small injection parameters B ($B \lesssim 3$–4). For large values of the mass transfer parameter, $5 \leqslant B \leqslant 100$, the following formula is suggested:

$$\frac{\tau_W}{\tau_W^0} = \left[\frac{\ln(1+B)}{B}\right]^{4/5}\left[\frac{1+1.3B+0.4B^2}{(1+B)(1+0.5B)^2}\right]^{1/5}. \tag{33}$$

Friction and heat exchange between the fuel layer and the wall can be determined from the relations

$$\tau_T = \mu_2\frac{u_W-u_0}{\varepsilon};$$

$$q_T = \frac{\lambda_2}{\varepsilon}(T_W-T_0) + \frac{\mu_2(u_W-u_0)^2}{\varepsilon}.$$

Equations similar to equations (32) and (33) can be used to estimate the influence of injection on the friction of droplets or particles during their interaction with the carrying phase.

In the presence of chemical reactions between fuel vapours and an oxidant near the phase interface, the energy released in combustion will influence the heat flux from the gas into the condensed phase. This effect can be taken into account by equation (29), since it allows for the release of chemical energy $W_1\Delta H$. Equations (28) and (31) need to be corrected for the case when combustion takes place in the diffusive microflame adjoining the surface of each particle

$$q_W = \frac{2\lambda_1}{\hat c_{p1}d}[\hat c_{p1}(T_1-T_W) + (Y_1-Y_{1W})Q_{pW}(T_W)] + \frac{\mu_1(u_1-u_W)^2}{d} \tag{34}$$

$$q_d = Nu_d\frac{\pi d_k\lambda_1}{\hat c_{p1}}[\hat c_{p1}T_1 - \hat c_{pW}T_W + (Y_1-Y_{1W})\phi_N\Delta H] \tag{35}$$

where, following ref. [45], the notation is: $Q_{pW}(T_W) = \Delta c_{pW}T_W + \phi_N\Delta H$ is the chemical reaction heat at the temperature T_W, ΔH the reaction heat at absolute zero, $\phi_j = m_j(v_j''-v_j')/m_1(v_1''-v_1')$ the stoichiometric ratio; m_j the molar mass of the jth component; v_j', v_j'' the stoichiometric coefficients before and after reaction.

The time of the start of intensive phase transition (t_e), when it is necessary to pass over to the formulae accounting for the influence of injection on friction and heat transfer, can be approximately determined from the phase interface temperature rise-up to some effective value T_{eff}. In many problems this value turns to be close to the boiling temperature T_b at the given pressure. The thus found conventional time of evaporation delay t_e can be determined by solving the second boundary-value heat conduction problem

$$T_{\text{eff}} - T_{20} = -\frac{1}{\sqrt{(\lambda_2\rho c_2\pi)}}\int_0^{t_e}\frac{q^0(\eta)}{\sqrt{(t_e-\eta)}}\,d\eta. \tag{36}$$

The presence of a diffusive microflame around a particle is given by the condition

$$T_1 \geqslant T_*;\quad Y_1 \geqslant Y_* \tag{37}$$

where T_* is the ignition temperature. As shown experimentally, the time of ignition delay t_{ind} depends on the temperature T_1 and does not depend on the concentration Y_1 when equation (37) is satisfied.

The mass transfer rate $\dot m$ for a film and droplets can be determined using the results of refs. [31, 32, 44, 45]

$$\dot{m}_d = \begin{cases} \dfrac{2\lambda_1}{\hat{c}_p d_k}\ln\left[1+\dfrac{1}{h_L}(\hat{c}_{p1}T_1-\hat{c}_{pW}T_W+(Y_1-Y_{1W})\phi_N\Delta H)\right](1+0.276Re_d^{1/2}\,Pr^{1/3}); & T_1 \geqslant T_* \\ \dfrac{2\lambda_1}{\hat{c}_p d_k}\ln\left[1+\dfrac{1}{h_L}(\hat{c}_{p1}T_1-\hat{c}_{pW}T_W)\right](1+0.276Re_d^{1/2}\,Pr^{1/3}); & T_1 < T_* \end{cases} \quad (38)$$

$$\dot{m}_W = \frac{q_W}{h_L+c_2(T_W-T_2)}$$

$$\dot{m}_f = \begin{cases} k_1\varepsilon\dfrac{\surd(\rho\rho_1)(u_1-u_W)(u_W-u_0)}{\sigma}\left(\dfrac{\rho}{\rho_1}\right)^{0.5}\left(\dfrac{T_1}{T_W}\right)^{0.25}-k_2Re_2; & We > We_* \\ 0; & We \leqslant We_* \end{cases} \quad (39)$$

$$We_* = \max\left\{5;\frac{k_2}{k_1}\left(\frac{\rho_1}{\rho}\right)^{0.5}\left(\frac{T_W}{T_1}\right)^{0.25}Re_2\right\};\quad k_1 = 10^{-4}\,\mathrm{kg\,m^{-2}\,s^{-1}};\quad k_2 = 0.4\times10^{-4}\,\mathrm{kg\,m^{-2}\,s^{-1}}$$

where σ is the coefficient of surface tension; $We = (\rho\rho_1)^{0.5}(u_1-u_W)(u_W-u_0)\varepsilon\sigma^{-1}$ the Weber number; We_* the critical Weber number at which the instability of the film surface sets in [48]. The semi-empirical equation (39) is obtained by processing the data of refs. [32, 50]. The instantaneous diameter of droplets can be determined as $d_k = (6\alpha_3/(\pi n))^{-1/3}$; $Re_2 = \rho(u_W-u_0)\varepsilon/\mu_2$. The fuel surface velocity is $u_W = 2u_2-u_0$.

5. CALCULATIONS

As an example consider the development of detonation in heterogeneous systems with a small volumetric content of a condensed phase and rather fine droplets (<200 μm): $\alpha_2 \ll 1$, $\alpha_3 \ll 1$, $A_0 \approx A$. The liquid film is considered stationary in the first approximation $u_2 = 0$, the atomization of droplets is absent (the Weber numbers for droplets are several orders smaller than for a film). In this case the system of equations has the form

$$\frac{\partial\rho_1}{\partial t}+\frac{\partial\rho_1u_1}{\partial x} = I_W+I_d \quad (40a)$$

$$\frac{\partial\rho_1Y_j}{\partial t}+\frac{\partial\rho_1u_1Y_j}{\partial x} = W_j+Z_j/\Delta H + \begin{cases}0; & j\neq N\\ I_W+I_d; & j = N\end{cases} \quad (40b)$$

$$\frac{\partial\rho\alpha_2}{\partial t} = -I_W-I_f \quad (40c)$$

$$\frac{\partial\rho\alpha_3}{\partial t}+\frac{\partial\rho\alpha_3u_3}{\partial x} = I_f-I_d \quad (40d)$$

$$\frac{\partial\rho\alpha_3u_3}{\partial t}+\frac{\partial\rho\alpha_3u_3^2}{\partial x} = F_d-I_du_3 \quad (40e)$$

$$\frac{\partial\rho_1u_1}{\partial t}+\frac{\partial\rho_1u_1^2}{\partial x}+\frac{\partial p_1}{\partial x} = -F_W-F_f-F_d+I_du_3 \quad (40f)$$

$$\frac{\partial\rho_1(\hat{e}_1+u_1^2/2)}{\partial t}+\frac{\partial\rho_1u_1(\hat{e}_1+u_1^2/2)}{\partial x}+\frac{\partial p_1u_1}{\partial x} = W\Delta H-Q_W-Q_d+(I_W+I_d)\left(e_W+\frac{p_1}{\rho}\right) + Z+I_d\frac{u_3^2}{2}-F_du_3 \quad (40g)$$

$$p_1 = \rho_1RT\sum_{j=1}^{N}\frac{Y_j}{m_j};\quad \hat{e}_1 = \sum_{j=1}^{N}Y_jc_{vj}T_1;$$

$$W_j = -W\frac{\phi_j}{\phi_N}. \quad (40h)$$

In equations (40) the terms of the type $\rho_1\alpha_2$, $\rho_1\alpha_3$ are neglected, but the terms $\rho\alpha_2$ are preserved, since $\rho \gg \rho_1$. The shedding of droplets is calculated with the use of the relation

$$(u_W-u_0)_2 = \frac{\tau_W\varepsilon}{\mu_2}.$$

When solving the problem, it is convenient to present the set of equations (40) in vector form

$$\frac{\partial\mathbf{X}}{\partial t}+\frac{\partial}{\partial x}\mathbf{A}(\mathbf{X}) = \mathbf{D}(\mathbf{X}) \quad (41)$$

where **X**, **A(X)**, **D(X)** are the columns prescribed by the equalities

$$\mathbf{X} = \begin{Bmatrix} \rho_1 \\ \rho_1Y_j \\ \rho\alpha_2 \\ \rho\alpha_3 \\ \rho_1u_1 \\ \rho_3\alpha_3u_3 \\ \rho_1\left(\hat{e}_1+\dfrac{u_1^2}{2}\right) \end{Bmatrix}$$

$$\mathbf{A}(\mathbf{X}) = \begin{Bmatrix} \rho_1u_1 \\ \rho_1u_1Y_j \\ 0 \\ \rho\alpha_3u_3 \\ \rho_1u_1^2+p_1 \\ \rho_3\alpha_3u_3^2 \\ \rho_1u_1\left(e_1+\dfrac{u_1^2}{2}+\dfrac{p_1}{\rho_1}\right) \end{Bmatrix}$$

$$\mathbf{D}(\mathbf{X}) = \left\{\begin{array}{l} I_W + I_d \\ W_j + Z_j/\Delta H + \begin{cases} 0; j \neq N \\ I_W + I_d; j = N \end{cases} \\ -I_W - I_f \\ I_f - I_d \\ -F_W - F_f - F_d + I_d u_3 \\ F_d - I_d u_3 \\ I_d \dfrac{u_3^2}{2} - F_d u_3 + W\Delta H - Q_W - Q_d \\ \quad + (I_W + I_d)\left(e_W + \dfrac{p_1}{\rho}\right) + Z \end{array}\right\}.$$

The system of equations (41) can be solved with the use of a two-step differential scheme of Lax–Wendroff. In this paper its modification is employed. In the absence of phase interactions ($\mathbf{D} \equiv 0$) the scheme has the form

first step:

$$\mathbf{X}_{j+1/2}^{n+1/2} = \tfrac{1}{2}(\mathbf{X}_{j+1}^{n} + \mathbf{X}_{j}^{n}) - \frac{\Delta t}{\Delta x}\tfrac{1}{2}(\mathbf{A}_{j+1}^{n} - \mathbf{A}_{j}^{n})$$

second step:

$$\mathbf{X}_{j}^{n+1} = \mathbf{X}_{j}^{n} - \frac{\Delta t}{\Delta x}(\mathbf{A}_{j+1/2}^{n+1/2} - \mathbf{A}_{j-1/2}^{n+1/2}).$$

The scheme has second-order accuracy, the condition of stability is the Courant condition

$$\Delta t \leqslant \frac{\Delta x}{\max_j(|u| + a)}$$

where a is the local speed of sound.

The account for phase interactions is made with the use of the third step

$$\mathbf{X}_{j}^{n+1} = \mathbf{X}_{j}^{n+1} + \Delta t \cdot \mathbf{D}(\mathbf{X}_{j}^{n+1}).$$

The oscillations of numerical solution can be suppressed by the layer-by-layer smoothing procedure

$$\mathbf{X}_{j}^{n} = (1 - 2\zeta)\mathbf{X}_{j}^{n} + (\mathbf{X}_{j+1}^{n} + \mathbf{X}_{j-1}^{n}); \quad 0 < \zeta < \tfrac{1}{2}.$$

Figure 3 presents an example calculation of the pressure profile variation along a closed tube length ($d = 4$ cm) for detonation propagation in a two-phase system of the gas–film type ($\alpha_{30} = 0$). Air was assumed to be an oxidant, n-decane a fuel. Detonation was initiated by a shock wave originating during the breakdown of the initial discontinuity. In actual practice this corresponds to detonation initiation in a shock tube on membrane rupture. The dashed curves show the initial distributions of the parameters given by exact solution of the problem on the breakdown of discontinuity in a non-reactive ideal gas. It is seen from the figure that an originating shock wave is accelerated by additional energy release after the ignition of a combustible mixture formed behind the wave. Secondary waves, originating in the zone of intensive fuel shedding from the crests of waves and mixing with the oxidant, overtake the bow shock wave and enhance it. The results of further calculations showed that, after the interaction between the second and the bow shock waves, the intensity of the latter gradually decreases. In this case the mean velocity of the detonation complex remains constant and independent, beginning from some time instant, of the initiation and boundary conditions on the left end of the tube. The results of velocity calculations of the self-sus-

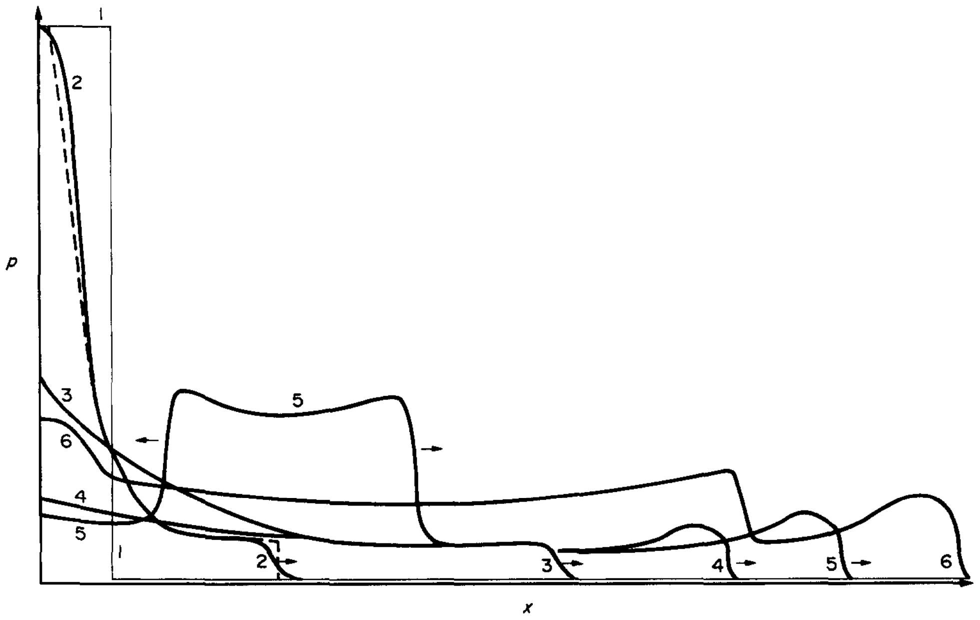

FIG. 3. Pressure profiles along the tube length at different time instants on heterogeneous detonation initiation after bursting of the diaphragm in a shock tube.

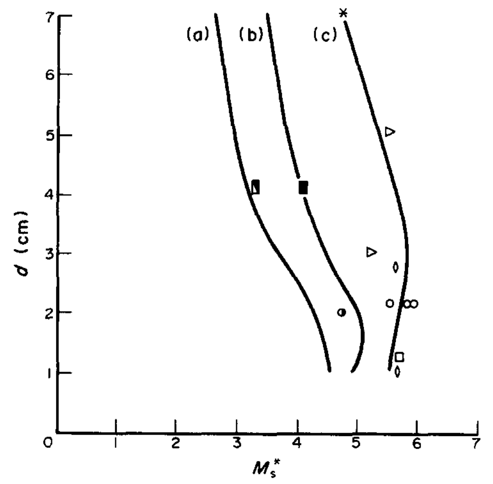

FIG. 4. Dependence of the pulsing self-sustaining detonation velocity on the tube diameter d and the fraction of the inner surface wetted with fuel: (a) quarter of the inner surface is covered by fuel ($\Pi_T/(\Pi_0+\Pi_T) = \frac{1}{4}$); (b) half the inner surface is covered by fuel; (c) the entire inner surface is covered by fuel.

taining mode (Fig. 4) and of the acceleration dynamics up to the attainment of stable conditions (Fig. 5) are in good agreement with the experimental data of refs. [3–5, 11, 12, 19]. Figure 4 presents the results of calculation of the velocities for self-sustaining modes of heterogeneous detonation propagation. For comparative purposes, the figures contain experimental data of different authors. It is seen from the figures that the dependence of the detonation rate on the tube diameter has essentially non-monotonous character. An increase in the self-sustaining detonation rate with a reduction of the transverse dimension of the channel is caused by the rise of the mean density of energy release behind the bow wave in fuel surface combustion and secondary explosions. With a further contraction of the channel, the increase of the friction and heat removal losses exceeds the increase in the mean density of energy release, thus leading to a smaller velocity of the self-sustaining mode.

In Fig. 5 the plots of the detonation rate Mach numbers in non-mixed two-phase systems vs time are presented. The calculation is made for the case when an oxidant is oxygen, a fuel is n-decane, $p_0 = 1$ atm and $T^0 = 300$ K. Solid lines correspond to the case when the fuel covers half the tube inner surface, dashed lines when the fuel covers one-fourth of the tube inner surface. The graph $M_S(t) = D/a_0$ for each case consists of two branches (increasing and decreasing) that converge with time to the rate of self-sustaining detonation $M_S(t) \rightarrow M_S^*$.

The results of calculations can be compared with the experimental data on the basis of the results of ref. [11]. In a square cross-section (0.41 m) tube with two walls wetted by fuel the rate of the experimentally observed detonation increased from 1200 to 1370 m s^{-1} at a distance of 1 m and then remained virtually unchanged. The calculations show (Fig. 5) that the increase in the velocity from 1200 m s^{-1} up to the constant, on average, velocity of 1420 m s^{-1} takes place over a distance of 1.25 m.

The calculation of the dependence of the self-sustaining detonation velocity on the initial oxygen concentration in the oxidant Y_{10} (Fig. 6) shows that the velocity D decreases with Y_{10}. The experimental data of ref. [12] fall well on the predicted curve.

In some calculations, seal failure of the left end was

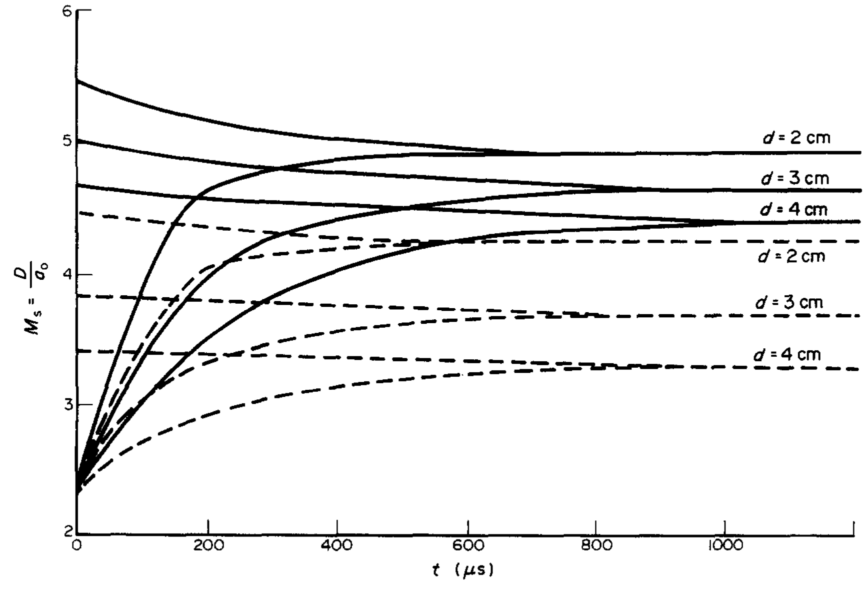

FIG. 5. Variation of the heterogeneous detonation velocity with time over the unsteady stage of development.

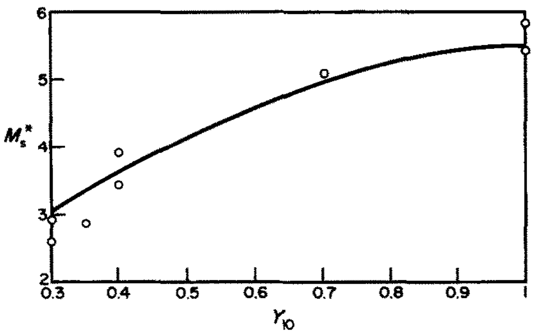

FIG. 6. Dependence of the heterogeneous detonation velocity on the oxygen initial concentration (fuel—liquid n-decane): $T_0 = 300$ K; $p_0 = 10^5$ MPa; $d = 2.2$ cm.

modelled as

$$u_{x=-x_0} = 0; \qquad t \leqslant t_g$$

$$p_{x=-x_0} = p_0; \qquad t > t_g.$$

Whenever the self-sustaining mode was attained when $t < t_g$, the seal failure did not influence the velocity of the detonation complex.

The experimental investigations conducted by the author made it possible to obtain (Fig. 7) an oscillogram of pressure variation with time for detonation acceleration in a dispersed mixture of diesel fuel with air (tube diameter $d = 50 \times 10^{-3}$ m, diameter of droplets $d_k = 0.2 \times 10^{-3}$ m). The space between the gauges is 0.5 m, the time of scanning is $t_p = 2 \times 10^{-3}$ s grad^{-1}. It is seen from the figure that the velocity of the bow shock wave increases from 450 to 900 m s^{-1}. In this case the fourth gauge records the origination of the secondary shock wave.

Thus, the proposed method of calculation allows the modelling, with sufficient accuracy, of the dynamics of detonation development in two-phase systems and the determination of the velocity of a self-sustaining mode.

REFERENCES

1. T. V. Vilensky and D. M. Khzmalyan, *Dynamics of Pulverized Fuel Combustion.* Izd. Energiya, Moscow (1978).
2. R. M. Clayton and S. Rogero, Experimental measurements on a rotating detonation-like wave observed during liquid rocket resonant combustion, 7th Liquid Propulsion Symp., Denver, Colorado, October (1965).
3. E. K. Dabora, K. W. Ragland and J. A. Nicholls, A study of heterogeneous detonations, *Astronautica Acta* **12**(1), 9–16 (1966).
4. V. E. Gordeyev, V. F. Komov, A. I. Serbinov and Ya. K. Troshin, On explosions in air piston compressors and manifolds, *Promysh. Energ.* **19**(12), 24–29 (1964).
5. E. K. Dabora, K. W. Ragland and J. A. Nicholls, Drop-size effects in spray detonations, 12th Symposium (Int.) on Combustion, New York, pp. 19–26 (1968).
6. C. W. Kauffman and J. A. Nicholls, Shock-waves ignition of liquid fuel drops, *AIAA J.* **9**(5), 880–885 (1971).
7. S. A. Zhdan, Estimation of the energy of spray detonation initiation, *Fiz. Goren. Vzryva* **20**(6), 138–141 (1984).
8. Yu. A. Nikolayev and P. A. Fomin, A model of steady-state heterogeneous detonation in a gas–droplet medium, *Fiz. Goren. Vzryva* **20**(4), 97–105 (1984).
9. R. Loison, Propagation d'une deflagration dans une tube reconvert d'une pellicule d'huit, *C. R. Acad. Sci.* **234**(5), 512–513 (1959).
10. V. F. Komov and Ya. K. Troshin, On the properties of detonation in some heterogeneous systems, *Dokl. Akad. Nauk SSSR* **175**(1), 109–112 (1967).

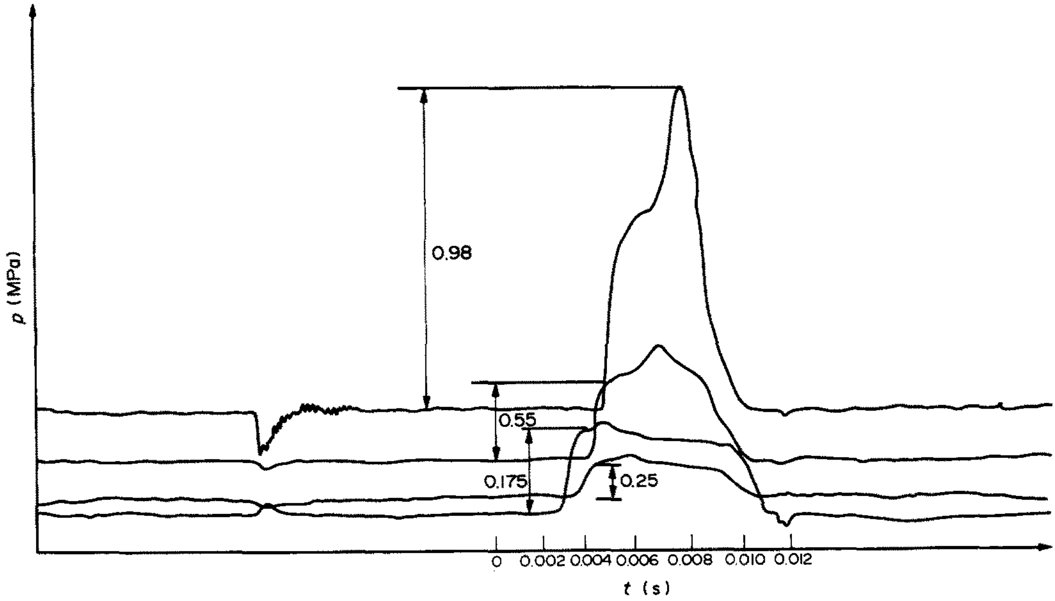

FIG. 7. Oscillograms of pressure variation in four gauges on detonation acceleration in a dispersed mixture of diesel fuel with air.

11. K. W. Ragland and J. A. Nicholls, Two-phase detonation of a liquid layer, *AIAA J.* 7(5), 859–863 (1969).
12. K. W. Ragland and C. F. Garcia, Ignition delay measurements in two-phase detonation, *Combustion Flame* **18**(1), 53–58 (1972).
13. I. N. Zverev and N. I. Zverev, *Detonation in Non-premixed Heterogeneous Systems* (Collected Papers), pp. 50–57. Izd. MGU, Moscow (1975).
14. I. N. Zverev, V. M. Gendugov and N. I. Zverev, Detonation of heterogeneous systems of non-premixed phases, *Fiz. Goren. Vzryva* No. 6, 903–909 (1975).
15. N. I. Zverev and N. N. Smirnov, The development of detonation in non-mixed two-phase systems, *Vestnik Moskov. Univ.*, Ser. 1, *Mat. Mekh.* No. 6, 82–87 (1979).
16. V. V. Mitrofanov and A. V. Pinaev, Spin detonation in heterogeneous systems of gas–film type, *Dokl. Akad. Nauk SSSR* **225**(3), 613–616 (1975).
17. A. P. Boychenko, N. I. Zverev, N. N. Smirnov and S. A. Kurnikov, Combustion to detonation transition in gasoline–air and solar oil–air dispersed mixtures. In *Physics of Aerodispersed Systems* (Collected Papers), No. 30, pp. 85–92. Kiev (1986).
18. S. S. Rybanin, One-dimensional model of detonation of heterogeneous systems, *Dokl. Akad. Nauk SSSR* **168**(4), 857–859 (1966).
19. S. A. Lesnyak, M. A. Nazarov, Ya. K. Troshin and K. I. Shchyolkin, Concerning the mechanism of heterogeneous detonation propagation, *Dokl. Akad. Nauk SSSR* **182**(5), 628–631 (1968).
20. A. A. Borisov, S. M. Kogarko and A. V. Lyubimov, On the instability of fluid surface with detonation and shock waves sliding on it, *Dokl. Akad. Nauk SSSR* **164**(1), 125–126 (1965).
21. A. A. Borisov, S. M. Kogarko and A. V. Lyubimov, Sliding of detonation and shock waves on fluid surface, *Fiz. Goren. Vzryva* No. 4, 31–38 (1965).
22. A. A. Borisov, S. M. Kogarko and A. V. Lyubimov, Ignition of fuel films behind shock waves in air and oxygen, *Combustion Flame* **12**(5), 465–468 (1968).
23. S. A. Lesnyak, M. A. Nazarov, Ya. K. Troshin and K. I. Shchyolkin, Interaction between a shock wave and a viscous liquid film, *Dokl. Akad. Nauk SSSR* **183**(3), 628–629 (1968).
24. S. A. Lesnyak, M. A. Nazarov, A. I. Serbinov and Ya. K. Troshin, On ignition delay in the front of heterogeneous (gas–film) detonation, *Fiz. Goren. Vzryva* **11**(6), 896–902 (1975).
25. M. V. Vorobiyov, S. A. Lesnyak, M. A. Nazarov and Ya. K. Troshin, Viscous liquid film destruction by a shock-compressed gas flow, *Dokl. Akad. Nauk SSSR* **230**(2), 344–346 (1976).
26. M. V. Vorobiyov, S. A. Lesnyak, M. A. Nazarov, V. G. Slutsky and Ya. K. Troshin, Heterogeneous (gas–film) detonation. In *Chemical Physics of the Processes of Combustion and Detonation. Detonation*, pp. 86–92. Chernogolovka (1977).
27. A. A. Borisov, B. E. Gelfand, S. M. Sherpanev and E. I. Timofeyev, On the mechanism of mixture formation behind a shock wave sliding along the liquid fuel surface, *Fiz. Goren. Vzryva* **17**(5), 86–92 (1981).
28. V. M. Gendugov, Diffusion flame in a turbulent boundary layer behind a shock wave sliding along the liquid fuel surface, *Fiz. Goren. Vzryva* **15**(2), 41–45 (1979).
29. S. A. Lesnyak, V. G. Slutsky and Ya. K. Troshin, Diffusional model of heterogeneous (gas–film) detonation. In *Combustion and Explosion*, pp. 469–474. Izd. Nauka, Moscow (1977).
30. V. M. Gendugov, On the structure of detonation waves in heterogeneous systems with non-premixed phases, *Fiz. Goren. Vzryva* **15**(5), 124–127 (1979).
31. S. M. Frolov, B. E. Gelfand and E. I. Timofeyev, Interaction between a liquid film and a high-speed gas flow behind a shock wave, *Fiz. Goren. Vzryva* **20**(5), 107–114 (1984).
32. S. M. Frolov, B. E. Gelfand and A. A. Borisov, A simple model of detonation in the system gas–film with account for mechanical entrainment of fuel, *Fiz. Goren. Vzryva* **21**(1), 110–117 (1985).
33. M. Sichel, C. S. Rao and J. A. Nicholls, A simple theory for the propagation of film detonation, 13th Symposium (Int.) on Combustion, Univ. Utah, Salt Lake City, Utah, pp. 1141–1149 (1970).
34. C. S. Rao, M. Sichel and J. A. Nicholls, Two-dimensional theory for two-phase detonation of liquid films, *Combustion Sci. Technol.* **4**(5), 209–216 (1972).
35. J. Futjusuma and S. Tsuge, On detonation waves supported by diffusion flames, 14th Symposium (Int.) on Combustion, Univ. Pennsylvania, pp. 1265–1275 (1972).
36. S. A. Lesnyak, V. G. Slutsky and Ya. K. Troshin, Influence of oxidant composition on the rate of heterogeneous (gas–film) detonation, *Fiz. Goren. Vzryva* **11**(5), 589–596 (1975).
37. V. F. Pleshakov, N. A. Shchepotiev and B. A. Ivanov, The mechanism of the limits of flame propagation in heterogeneous systems lubricant film–gaseous oxidant, *Fiz. Goren. Vzryva* **12**(1), 37–47 (1976).
38. V. M. Gendugov, On detonation in heterogeneous systems with non-premixed phases, *Fiz. Goren. Vzryva* **18**(3), 117–120 (1982).
39. S. A. Lesnyak and V. G. Slutsky, Heterogeneous (gas–film) detonation. The rule for selecting velocities in fuel-superenriched systems, *Fiz. Goren. Vzryva* **20**(4), 90–96 (1984).
40. T. V. Ramodanova and I. N. Zverev, Two-phase detonation in tubes (oxidant in the volume–fuel on the walls). In *Gas and Wave Dynamics*, No. 2, pp. 155–158. Izd. MGU, Moscow (1979).
41. N. I. Zverev and N. N. Smirnov, Structure and properties of heterogeneous detonation. In *Interaction Between Waves in Deformed Media*, pp. 56–71. Izd. MGU, Moscow (1984).
42. I. N. Zverev, N. I. Zverev and N. N. Smirnov, Detonation in heterogeneous systems gas–film. In *Gas and Wave Dynamics*, No. 3, pp. 91–99. Izd. MGU, Moscow (1979).
43. N. N. Smirnov, Spin detonation in a two-phase system gas–film, *Vestnik Moskovsk. Univ.*, Ser. 1, *Mat. Mekh.* No. 2, 81–86 (1980).
44. N. I. Zverev and N. N. Smirnov, Two-phase detonation above a fuel layer, *Fiz. Goren. Vzryva* **18**(1), 143–145 (1982).
45. N. N. Smirnov, Heat and mass transfer in a multi-component chemically reactive gas above a liquid fuel layer, *Int. J. Heat Mass Transfer* **28**(5), 929–938 (1985).
46. N. N. Smirnov, Heat and mass transfer unsteady diffusion combustion of the condensed fuel surface, *Int. J. Heat Mass Transfer* **29**(3), 673–679 (1986).
47. R. I. Nigmatulin, Dynamics of heterogeneous media. Preprint of the Institute of Thermophysics of the Siberian Branch of the USSR Academy of Sciences, Novosibirsk (1984).
48. R. I. Nigmatulin, *Fundamentals of Mechanics of Heterogeneous Media*. Izd. Nauka, Moscow (1978).
49. N. N. Smirnov, Fuel layer combustion with surface blowing by an oxidant flow, *Fiz. Goren. Vzryva* **18**(5), 63–70 (1982).
50. B. I. Nigmatulin, L. A. Klebanov and A. E. Kroshilin, Burnout heat transfer in vapour–liquid dispersed–annular flows under unsteady-state conditions, *Teplofiz. Vysok. Temp.* No. 6, 63–70 (1980).

COMBUSTION ET DETONATION DANS UN MILIEU MULTIPHASIQUE—INITIATION DE LA DETONATION DANS LES SYSTEMES DISPERSES OU A FILM, DERRIERE UNE ONDE DE CHOC

Résumé—On considère les problèmes de la propagation de combustion et de détonation dans les milieux hétérogènes contenant un oxydant dans la phase gazeuse et un combustible dans la phase condensée sous la forme de particules dispersées dans l'écoulement oxydant ou d'un film mince sur les parois du canal. La détonation dans de tels systèmes a une structure variable, complexe, nettement différente de la monidimensionnalité: le front de détonation peut montrer des discontinuités mobiles et il peut être périodiquement pulsé. Un modèle physique de détonation pulsatoire et tournante est développé pour les milieux hétérogènes. Un système clos d'équations avec des conditions aux limites permet la simulation mathématique de la transition entre la combustion lente et la détonation. Le mécanisme de transition et les paramètres déterminants de la détonation sont calculés numériquement. On étudie expérimentalement les mécanismes variables de la transition de la combustion dans les mélanges dispersés d'air avec un hydrocarbure combustible.

VERBRENNUNG UND EXPLOSION IN EINEM MEHRPHASENGEMISCH—ZÜNDUNG DER EXPLOSION IN EINEM DISPERSEN FILM HINTER EINER SCHOCKWELLE

Zusammenfassung—In dieser Arbeit wurde die Ausbreitung der Verbrennung und der Explosion in einem heterogenen Medium untersucht. In diesem Gemisch liegt das Oxidationsmittel als Gas vor, und der Brennstoff befindet sich entweder als feiner Film an der Rohrwand oder als dispers verteilte Partikel in dem Oxidationsmittelstrom. Die Explosion in einem solchen System ist ein komplexer, dynamischer Vorgang, der keinesfalls eindimensional beschrieben werden kann. Die sich vorwärtsbewegende Explosionsfront stellt sich als diskontinuierliche Bewegung dar und kann periodisch pulsieren. Ein physikalisches Modell der pulsierenden und drehenden Explosionsfront in einem heterogenen Gemisch wurde entwickelt. Ein geschlossenes System von Gleichungen mit den zugehörigen Randbedingungen wurde aufgestellt. Damit können die Vorgänge, angefangen bei der langsamen Verbrennung bis zur Explosion, mathematisch simuliert werden. Die Parameter, die den Prozeß im Übergangsbereich zwischen Verbrennung und Explosion bestimmen, wurden numerisch berechnet. Der dynamische Prozeß zwischen Verbrennung und Explosion in dispersen Gemischen von Luft und brennbarem Kohlenwasserstoff wurde experimentell untersucht.

ГОРЕНИЕ И ДЕТОНАЦИЯ В МНОГОФАЗНЫХ СРЕДАХ. ИНИЦИИРОВАНИЕ ДЕТОНАЦИИ В ДИСПЕРСНО-ПЛЕНОЧНЫХ СИСТЕМАХ ЗА УДАРНОЙ ВОЛНОЙ

Аннотация—В работе рассматриваются задачи распространения горения и детонации в гетерогенных средах, содержащих окислитель в газообразной фазе и горючее в конденсированной фазе в виде дисперсированных частиц в потоке окислитедя или тонкой пленки на стенках канала. Показано, что детонация в таких системах обладает сложной существенно неодномерной нестационарной структурой: передний фронт детонации может содержать подвижные изломы и периодически пульсировать. Разработана физическая модель пульсирующей и спиновой детонации в гетерогенных средах. Составлена замкнутая система уравнений с граничными условиями, позволяющая провести математическое моделирование перехода медленного горения в детонацию. Проведены численные расчеты процесса перехода и определяющих параметров детонации. Экспериментально исследованы нестационарные процессы перехода горения в детонацию в дисперсных смесях воздуха с углеводородным горючим.